Published in final edited form as:
Proteins. 2008 June ; 71(4): 1779–1791. doi:10.1002/prot.21859.

Functional and computational studies of the ligand-associated metal binding site of β3 integrins

Marta Murcia[1,2], **Marketa Jirouskova**[3], **Jihong Li**[3], **Barry S. Coller**[3], and **Marta Filizola**[1,2,*]

1 *Department of Structural and Chemical Biology, Mount Sinai School of Medicine, New York, New York 10029*

2 *Department of Physiology and Biophysics, Weill Medical College of Cornell University, New York, New York 10021*

3 *Laboratory of Blood and Vascular Biology, The Rockefeller University, New York, New York 10021*

Abstract

A combination of experimental and computational approaches was used to provide a structural context for the role of the β3 integrin subunit ligand-associated metal binding site (LIMBS) in the binding of physiological ligands to β3 integrins. Specifically, we have carried out (1) adhesion assays on cells expressing normal αIIbβ3, normal αVβ3, or the corresponding β3 D217A LIMBS mutants; and (2) equilibrium and nonequilibrium (steered) molecular dynamics (MD) simulations of eptifibatide in complex with either a fully hydrated normal αIIbβ3 integrin fragment (αIIb β-propeller and the β3 βA (I-like), hybrid, and PSI domains) or the equivalent β3 D217A mutant. Normal αIIbβ3 expressing cells adhered to immobilized fibrinogen and echistatin, whereas cells expressing the αIIbβ3 D217A LIMBS mutant failed to adhere to either ligand. Similarly, the equivalent αVβ3 mutant was unable to support adhesion to vitronectin or fibrinogen. The αIIbβ3 D217A mutation increased the binding of mAb AP5, which recognizes a ligand-induced binding site (LIBS) in the β3 PSI domain, indicating that this mutation induced allosteric changes in the protein. Steered MD simulating the unbinding of eptifibatide from either normal αIIbβ3 or the equivalent β3 D217A mutant suggested that the reduction in ligand binding caused by the LIMBS mutant required the loss of both the LIMBS and the metal ion-dependent adhesion site (MIDAS) metal ions. Our computational results indicate that the LIMBS plays a crucial role in ligand binding to αIIbβ3 by virtue of its effects on the coordination of the MIDAS.

Keywords

AP5; αIIbβ3; αVβ3; fibrinogen; molecular dynamics; steered molecular dynamics; binding; platelets

INTRODUCTION

Metal ions play an important role in integrin function, with complex effects on integrin activation, affinity for ligand, and ability to support rolling, firm adhesion, and/or aggregation of cells.[1–11] The crucial role of the MIDAS in the β3 (I-like) domain of αIIbβ3 in ligand binding was inferred from studies of naturally occurring mutations in select patients with the inherited hemorrhagic disorder Glanzmann thrombasthenia, as well as both site-directed and random mutations.[12–14] The crystal structures of both αVβ3 and αIIbβ3 confirmed the

*Correspondence to: Marta Filizola, Department of Structural and Chemical Biology, Mount Sinai School of Medicine, Icahn Medical Institute Building, Room 16–20, 1425 Madison Avenue, Box 1677, New York, NY 10029-6574. E-mail: E-mail: marta.filizola@mssm.edu.

presence of a MIDAS metal ion (although with some differences in the coordinating residues from those previously predicted) and provided an explanation for its role in ligand binding, since a carboxyl group oxygen of the Asp residue in the ligands analyzed interacted directly with the MIDAS metal ion.[5,8] Two additional metal ions were found in close proximity to the MIDAS in the β3 βA (I-like) domain in both αVβ3 and αIIbβ3 crystal structures; one was designated the ADMIDAS because it was adjacent to the MIDAS and the other was designated the LIMBS because it did not fill when αVβ3 was crystallized in the presence of either Ca^{2+} or Mn^{2+}, but it did fill with Mn^{2+} when the Ca^{2+} crystal was soaked with Mn^{2+} and a peptide ligand [cyclo(RGDf-*N*-*Me*V), cilengitide].[4,5] The LIMBS, the subject of this study, was filled with Ca^{2+} in the αIIbβ3 crystals, which were prepared in the presence of Ca^{2+}, Mg^{2+}, and one of several ligand mimetics or a pseudoligand.[8]

The LIMBS has been implicated as a positive regulator of ligand or ligand-mimetic antibody binding, but with variable effects in different integrins.[5,7–11,13–18] In the integrin β3 subunit, which is common to both αVβ3 and αIIbβ3, the residues involved in coordinating its metal ion are D158 (carboxyl oxygen), N215 (amide oxygen), D217 (carboxyl and carbonyl oxygens), P219 (carbonyl oxygen), and E220 (carboxyl oxygen); the latter also coordinates the MIDAS via its other carboxyl oxygen.[5,8] Chen *et al.* observed that an alanine mutation affecting the β7 LIMBS equivalent to β3 D217A had only a minor effect on the adhesion of cells expressing α4β7 to its immobilized ligand MAdCAM at low shear stress in the presence of Ca^{2+} or Ca^{2+} and Mg^{2+}, although the cells were somewhat more likely to roll than remain firmly adherent.[7] Another LIMBS mutation (equivalent to β3 N215A) partially reduced adhesion and further decreased firm adhesion, but not nearly as much as mutations of the MIDAS (equivalent to β3 D119A and S121A), which essentially eliminated adhesion.[7] In contrast to the partial effects on ligand binding caused by LIMBS mutations in β7, Goodman and Bajt reported that alanine mutations in β2 LIMBS residues equivalent to β3 D217A and E220A essentially abrogated ligand binding to both αLβ2 (ICAM-1) and αMβ2 (iC3b).[15] Similarly Chen *et al.*,[11] followed by Cheng *et al.*,[18] confirmed and extended these findings by demonstrating that LIMBS mutations in β2 at positions equivalent to β3 N215 and D217 eliminated adhesion to ICAM-1 by cells expressing αLβ2.

In αIIbβ3, β3 LIMBS mutations D217A and E220A were reported by Tozer *et al.* to abolish the binding of the ligand mimetic monoclonal antibodies (mAbs) PAC1 and OPG2.[13] Similarly, using a chemical mutagenesis approach in CHO cells expressing a constitutively active form of αIIbβ3, Baker *et al.*[14] identified mutations that eliminated PAC1 binding, including the LIMBS mutants D217N, P219S, and both E220K and E220Q.[14] Yamanouchi *et al.*[17] reported that CHO cells expressing αIIb with the β3 LIMBS mutant N215A did not: (1) bind PAC1 or fibrinogen when stimulated by mAb PT25-2, (2) support adhesion to immobilized fibrinogen, or (3) bind fibrinogen when expressed with a constitutively active αIIb subunit. These authors also found that the LIMBS mutation eliminated the binding of fibrinogen and the ligand mimetic mAb (WOW1) to αVβ3. Most recently, Cheng *et al.*[18] demonstrated that a D217H mutation in β3 leads to loss of fibrinogen binding to αIIbβ3.

Pesho *et al.* studied cation and ligand binding to an isolated normal β3 βA (I-like) domain, as well as mutant forms of the domain affecting the MIDAS (D119A), ADMIDAS (D126A), and LIMBS (D217A).[10] They reported that mutations of the MIDAS, ADMIDAS, and LIMBS all dramatically decreased fibrinogen binding at either low or high Ca^{2+} concentrations.

In this study, we carried out functional and computational studies to understand better the role of LIMBS in the binding of physiological ligands to β3 integrins. Adhesion assays on cells expressing the αIIbβ3 D217A LIMBS indicated (1) loss of fibrinogen binding, and (2) increased binding of mAb AP5 at its PSI binding site. Functional studies with another LIMBS mutant (N215A) confirmed that the observed changes were not unique to a single mutation.

The functional data obtained for normal αIIbβ3 and the corresponding β3 D217A LIMBS mutant were rationalized using equilibrium and nonequilibrium (steered) molecular dynamics (MD) simulations of either a fully hydrated normal αIIbβ3 integrin fragment (αIIb β-propeller and the β3 βA (I-like), hybrid, and PSI domains) in complex with eptifibatide or the equivalent β3 D217A mutant.

MATERIALS AND METHODS

Experimental procedures

Antibodies and other materials—Monoclonal antibodies (mAbs) 10E5 (anti-αIIbβ3), 7E3 (anti-αIIbβ3 + αVβ3), and 7H2 (anti-β3) have been described previously[19–21] and were produced at National Cell Culture Center, Minneapolis, MN; mAb HIP8 (anti-αIIb) was from BD Biosciences (San Jose, CA); mAb 1990 (anti-αIIb) was from Chemicon (Temecula, CA); and the ligand-induced binding site (LIBS) antibody AP5 (anti-β3 PSI domain)[22] was a generous gift of Dr. Peter Newman, Blood Center of Southeastern Wisconsin. Bovine serum albumin (BSA) and G418 were from Fisher (Suwanee, GA); DMEM, RPMI, and trypsin (0.25% solution) were from Invitrogen (Carlsbad, CA). Echistatin was obtained from Sigma Chemical (St. Louis, MO) and fibrinogen from American Diagnostica (Stamford, CT); vitronectin was a generous gift from Dr. Deane Mosher (University of Wisconsin-Madison School of Medicine, Madison, WI).

Site-directed mutagenesis, cell culture, and transfection—Mutant β3 constructs were generated using Quik-Change XL Site-Directed Mutagenesis Kit (Stratagene, La Jolla, CA). Human β3 cDNA in the pcDNA3.1/Myc-His mammalian expression vector was used as the template (kindly provided by Dr. Junichi Takagi, Harvard University, Boston, MA). After mutagenesis, the mutant cDNA was used to transform XL-10 Gold ultracompetent cells as per the manufacturer's instructions (Stratagene; Cedar Crest, TX). Human embryonic kidney (HEK) 293 cells were transfected with normal αIIb cDNA (pEF1/V5 mammalian expression vector; also kindly provided by Dr. Junichi Takagi) and either normal or mutant β3 as previously described.[23] Stable cell lines were generated by G418 selection (0.8 mg/mL) for 14 days. αIIbβ3-expressing cell lines were sorted once or twice using mAb 10E5 to achieve high-level αIIbβ3 expression and then resorted using mAb HIP8 to ensure similar surface expression of αIIbβ3. After sorting, cells were grown in 10% serum-supplemented DMEM containing G418 (0.8 mg/mL).

CS-1 cells (kindly provided by Dr. David Cheresh, The University of California at San Diego, La Jolla, CA), which express αV but not β3, were transfected with β3 constructs as described earlier. Stable cell lines expressing normal or mutant αVβ3 receptors were sorted with mAb 7H2 to achieve similar levels of αVβ3 expression.

Binding of monoclonal antibodies and fluorescent fibrinogen—HEK293 cells were harvested with 0.25% trypsin, washed with HEPES-buffered modified Tyrode's solution (HBMT), pH 7.4 containing 2% BSA, and finally resuspended in HBMT with 2% BSA, 100 μ*M* Ca^{2+}, 50 μ*M* Mg^{2+}, to a final concentration of 5×10^6 cells/mL. For mAb binding studies, cells were incubated with $Alexa^{488}$-labeled antibodies for 30 min at 22°C and analyzed by flow cytometry (FACS Calibur, Becton Dickinson, Franklin Lakes, NJ) after dilution with HBMT buffer containing the same ions. For fibrinogen binding studies, cells were incubated with 200 μg/mL of $Alexa^{488}$-fibrinogen (Invitrogen) in the presence of 2 m*M* Ca^{2+}/1 m*M* Mg^{2+}, and the activating mAb AP5 (60 μg/mL) for 30 min at 37°C. Cells were then washed with HBMT containing 2 m*M* Ca^{2+}/1 m*M* Mg^{2+}, fixed with 0.5% paraformaldehyde, and analyzed by flow cytometry.

Adhesion to fibrinogen and echistatin under static and flow conditions— Harvested HEK293 and CS-1 cells were adjusted to a final count of 10^6/mL and supplemented with Ca^{2+} and Mg^{2+} ions 10 min prior to the experiment as indicated in the "Results" section. Cells were added to microtiter wells precoated with fibrinogen (50 μg/mL), echistatin (10 μg/mL), or vitronectin (5 μg/mL) and allowed to adhere for 1 h at 37°C. To assess the specificity of adhesion, samples were also tested in the presence of 10 m*M* EDTA, 100 μ*M* tirofiban, or the mAbs 7E3 or 10E5 (both at 20–30 μg/mL). Unattached cells were removed by washing three times with HBMT containing the same ions as used in the adhesion assay. The number of adherent cells was assessed by measuring their endogenous acid phosphatase activity as per Law *et al.*,[24] and expressed as the percentage of the number of cells expressing normal αIIbβ3 or αVβ3 that adhered under the same conditions.

Adhesion under flow condition was performed as per Chen *et al.*[7] with minor modifications. The Petri dish creating the bottom of the parallel plate perfusion chamber (GlycoTech, Gaithersburg, MD) was coated with fibrinogen (50 μg/mL) for 1 h at 22°C and then blocked with HBMT containing 2% BSA to prevent nonspecific interactions. The chamber was then assembled, prefilled with buffer, and mounted onto an inverted microscope (Olympus, IX51; Melville, NY). Cells expressing αIIbβ3 prepared as above in the presence of either 2 m*M* Ca^{2+}/1 m*M* Mg^{2+} or 0.5 m*M* Mn^{2+} were allowed to accumulate for 90 s at 0.15 dyne/cm^2. The number of adherent cells (defined as cells not moving more than one cell diameter in 3 s) per field using a 20× objective was recorded at the end of the accumulation period.

Statistical analysis of normally distributed data was performed on the means of the two sets of data using Student's *t*-test; on sets of data without equal variances, the Mann Whitney Rank Sum test was performed (Sigma Stat, SPSS Science, Chicago, IL).

Computational methods

Simulations were performed with the GROMACS program package[25,26] using the optimized potentials for liquid simulations all-atom (OPLS-AA) force-field. The parameters for the OPLS-AA potential energy function were extended to include the peptide mimetic ligand eptifibatide. Visualization and analysis of the trajectories were conducted by using VMD[27] and GROMACS tools.[26]

Molecular systems—The recently published crystallographic structure of the liganded αIIbβ3 integrin fragment (αIIb β-propeller and the β3 βA (I-like), hybrid, and PSI domains) in complex with eptifibatide (PDBID code: 1TY6[8]) was used as a starting conformation for the computational study on normal αIIbβ3 and the αIIbβ3 β3 D217A mutant. Specifically, the selected Asp residue D217 was mutated to alanine by manual modification of the original atom and residue name in the αIIbβ3 crystal structure. Original coordinates from the αIIbβ3 crystal structure were used for eptifibatide, 190 crystallographic water molecules, and the metal ions (Ca^{2+} at LIMBS and ADMIDAS, and Mg^{2+} at MIDAS); however, the glycerol molecules were replaced by water molecules. Each complex system (normal αIIbβ3 or D217A mutant) was immersed in a pre-equilibrated 10 nm × 10 nm × 17 nm rectangular box of simple point-charge (SPC) water molecules and neutralized with 13 or 12 sodium counterions, respectively. Energy minimization was carried out in two steps. First, all heavy atoms were restrained to their crystallographic positions using a harmonic potential (force constant equal to 1000 kJ/(mol nm^2), while surrounding water molecules were minimized and then subjected to 50 ps of MD simulations in the NPT isobaric-isotherm ensemble at 300 K and 1 bar. Second, the resulting systems were energy minimized without any restraints.

Molecular dynamics simulations—MD simulations of 20 ns were carried out on the initial structures of normal αIIbβ3 and its D217A mutant generated as described earlier using periodic

boundary conditions in an NPT ensemble (constant pressure and temperature). Coulomb and short-range neighbor list cutoffs were both set to 0.9 nm, whereas the Lennard-Jones cut-off was set to 1.2 nm. Electrostatic contributions to the energies and forces were calculated using the Particle-Mesh Ewald (PME) summation algorithm.[28] The interpolation order was set to 4 and the maximum spacing for the combined charge/potential grid was set to 0.12 nm. A time step of 2 fs was employed, and the pair lists were updated every 10 steps. The linear constraint solver (LINCS) algorithm[29] was used to preserve the bond lengths. The weak-coupling scheme proposed by Berendsen *et al.*[30] was used for temperature and pressure control. Specifically, a temperature of 300 K was maintained constant with a time constant of 0.1 ps. For the pressure, semi-isotropic coupling was used with the reference pressure set at 1.0 bar.

Steered molecular dynamics—To induce unbinding of eptifibatide from the binding site of normal αIIbβ3 and its β3 D217A mutant, we used constant velocity steered molecular dynamics (SMD), a nonequilibrium simulation method to study molecular recognition and mechanical properties of proteins.[31] The configurations obtained after 20 ns of MD simulation for normal αIIbβ3 and the D217A mutant were energy minimized using the steepest-descent algorithm to the tolerance of 100 kJ/(mol nm) with eptifiba-tide and the backbone of the protein fixed, and those used as starting points for the SMD simulations. SMD runs were carried out following a protocol similar to the one that was recently described by Craig *et al*. for the forced unbinding of the cyclic RGD peptide cilengitide from αVβ3 in the presence of Mn^{2+}.[32] Specifically, the center of mass of eptifibatide was pulled out of the shallow binding site of αIIbβ3 by harmonic restrain to a point moving with a constant velocity of 0.0005, 0.001, 0.002, or 0.0005 nm/ps (5, 10, 20, and 50 Å/ns) and a spring force constant of 2500 kJ/(mol nm^2) (approximately equivalent to 10 $k_BT/Å^2$). The pulling direction was given by the sum of two vectors, pointing from the Cα atoms of residue 452 of the αIIb subunit and residue 301 of the β3 subunit to the center of mass of the ligand, as calculated from the normal αIIbβ3. All the starting conformations were superimposed based on the fitting of the Cα atoms of the α chain (β-propeller) and β-A domain (residues 109–352) so the same pulling direction could be applied in all SMD simulations. It should be noted that in contrast to Craig *et al.*, we did not use the β3 terminal residue 440 for the definition of the direction vector, as in our simulations of the liganded forms of the integrin we observed that this residue fluctuates substantially; nevertheless, an equivalent direction was obtained by choosing the Cα of residue 301 of the β3 subunit, which remains stable during dynamics. Similarly to Craig *et al.'s* work for αVβ3, and to explore the effect of the different ions in the force-time curve and the major force peak, additional SMD simulations for both normal and β3 D217A mutant αIIbβ3 were conducted turning off the interaction with the MIDAS ion, the LIMBS ion, the ADMIDAS ion, or both the MIDAS and the LIMBS.

RESULTS

β3 LIMBS mutation results in increased constitutive binding of the LIBS mAb AP5 to αIIbβ3

A panel of antibodies was used to characterize expression of normal αIIbβ3 or the corresponding β3 D217A or N215 LIMBS mutant on the surface of human embryonic kidney (HEK) 293 cells by flow cytometry. mAbs HIP8 (anti-αIIb), 7H2 (anti-β3),[20] and 10E5 (anti-αIIbβ3),[21] all bound to the normal and mutant receptors in similar proportions (data not shown). As expected, the mAb AP5, which reacts preferentially with ligand-bound and EDTA-treated αIIbβ3 on platelets,[22] bound poorly to normal αIIbβ3, and the binding was increased eight-fold in the presence of EDTA (Table I). In contrast, in the absence of EDTA, more AP5 bound to each of the LIMBS mutants than to normal αIIbβ3 ($P < 0.001$ for both) and EDTA produced only a three-fold increase in binding.

β3 LIMBS mutation results in loss of ligand binding to αIIbβ3

Adhesion of cells expressing normal or mutant αIIbβ3 receptors to microtiter wells coated with either fibrinogen or echistatin (a RGD-containing snake venom[33,34]) was measured to assess the ability of the LIMBS mutants to bind ligand. Cells expressing normal αIIbβ3 adhered readily to wells coated with either ligand in the presence of 100 μ*M* Ca^{2+} and 50 μ*M* Mg^{2+} (see Fig. 1). Pretreatment of these cells with the αIIbβ3-specifc mAb 10E5 (20 μg/mL), or the αIIbβ3 inhibitor tirofiban (100 μ*M*) resulted in nearly complete inhibition of adhesion to both fibrinogen and echistatin. In sharp contrast, cells expressing the β3 D217A LIMBS mutant of αIIbβ3 failed to adhere to either of these ligands. The results were similar for the other LIMBS mutant (N215A) (data not shown). When the adhesion assay was performed in the presence of 2 mM Ca^{2+} and 1 mM Mg^{2+} the data were similar to those obtained in the presence of the lower divalent cation concentrations.

Adhesion of normal αIIbβ3-expressing cells to fibrinogen under flow conditions (shear force of 0.15 dyne/cm^2) resulted in the accumulation of 27 ± 8 stably adherent cells/field after 90 s of perfusion in the presence of 2 m*M* Ca^{2+} and 1 m*M* Mg^{2+} and 29 ± 11 cells/field in the presence of 0.5 m*M* Mn^{2+} ($n = 6$). In sharp contrast, not a single cell expressing either the D217A ($n = 1$) or the N215A LIMBS mutation ($n = 4$) achieved stable adhesion to immobilized fibrinogen under the same shear conditions.

We also studied the ability of normal and mutant αIIbβ3-expressing cells to bind soluble, fluorescent fibrinogen in the presence of mAb AP5, which induces ligand binding.[22] AP5 increased fibrinogen binding to cells expressing normal αIIbβ3 by 3.4-fold (Table II), and this binding was judged to be specific for αIIbβ3 since it could be completely blocked by the addition of the αIIbβ3-specific mAb 10E5. In sharp contrast, when AP5 was added, there was no increase in fibrinogen binding to either the β3 D217A or N215A mutant.

β3 LIMBS mutation results in loss of ligand binding to αVβ3

CS-1 cells expressing normal αVβ3 adhered readily to vitronectin-coated wells in the presence of 1 m*M* Mg^{2+} [Fig. 2(A)] or 0.5 m*M* Mn^{2+} (data not shown). The adhesion was inhibited by mAb 7E3 (20 μg/mL), which reacts with both αIIbβ3 and αVβ3.[19] In contrast, CS-1 cells expressing αVβ3 with the β3 D217A mutation failed to adhere to vitronectin in the presence of 1 m*M* Mg^{2+} [Fig. 2(A)]. CS-1 cells expressing normal αVβ3 did not adhere to fibrinogen in the presence of 1 m*M* Mg^{2+} (data not shown), but did adhere to fibrinogen in the presence of 0.5 m*M* Mn^{2+} [Fig. 2(B)], and this adhesion was also inhibited by mAb 7E3. In contrast, the β3 D217A αVβ3 mutant bound poorly to fibrinogen in the presence of Mn^{2+}. Identical results were obtained with cells expressing the β3 LIMBS N215A mutant.

The dynamic behavior of the β3 D217A LIMBS mutant differs from normal αIIbβ3 during nanosecond time-scale MD simulations

Starting conformations of the normal αIIbβ3 integrin fragment or the corresponding β3 D217A LIMBS mutant were obtained according to the procedure described in the “Materials and Methods” section, and were simulated in rectangular boxes of 52,316 and 52,317 pre-equilibrated water molecules, respectively. Figure 3 shows the system setup created for normal αIIbβ3, which included the βA (I-like), hybrid, and PSI domains from the β3 subunit (residues 1–440) and the β-propeller from the αIIb subunit (residues 1–452) in complex with eptifibatide.[8] After neutralizing the net charge of the unit cells with sodium ions, the hydrated integrin fragments of both normal αIIbβ3 and the corresponding β3 D217A LIMBS mutant contained 171,172 atoms.

Simulations were run for 20 ns and their stabilities were checked by monitoring several time-dependent geometrical properties. Figure 4 shows the time evolution of the root mean-square

deviations (RMSD) of the Cα atoms of different domains of normal αIIbβ3 (black line) and the β3 D217A mutant (gray line) from the starting structure. As shown, the entire simulated protein system, as well as its individual subunits and domains appear to be equilibrated after 10 ns. The αIIb β-propeller domain [Fig. 4(B)] and the β3 βA (I-like) domain [Fig. 4(C)] did not deviate very much from their initial structures during the 20 ns simulation period (average RMSD < 1.5 Å). The simulated β3 chain moved the most during the simulations [Fig. 4(D)] as a result of the motion of the hybrid and PSI domains. However, these domains maintained their global folding during the entire duration of the simulation as indicated by the time evolution of the total number of hydrogen bonds, the radius of gyration of the Cα atoms, and the total accessible surface area (data not shown). The conformation of the ligand mimetic cyclic peptide eptifibatide did not deviate significantly from its initial crystallographic structure during the simulations of either normal αIIbβ3 or the β3 D217A LIMBS mutant (data not shown).

β3 D217A LIMBS mutation produces changes in the LIMBS and MIDAS coordination spheres

The location of the normal and β3 D217A LIMBS mutant metal ions at the end of the 20 ns simulation of normal αIIbβ3 is shown in Figure 5. As can be seen in Figure 5(A), after the simulation of normal αIIbβ3, the orientation of the ligand Asp side-chain remained the same as in the αIIbβ3 crystal structure, with the carboxylic oxygen OD2 interacting with the MIDAS Mg^{2+} ion [Fig. 6(F), black line] and the other oxygen atom, OD1, forming hydrogen bonds with the backbone amine groups of Y122 and N215, and additional contacts with the aliphatic side-chain of R214 (data not shown).[8] The distance between the LIMBS metal ion (Ca^{2+}) and the ligand Asp oxygen atoms also remained constant during the 20 ns MD simulation of normal integrin αIIbβ3 [Fig. 6(A,B), black line]. The only significant contact change between the β3 metal ions and protein side chains during the MD simulation of normal integrin αIIbβ3 involved the rapid increase in the distance between MIDAS metal ion and the carboxylic oxygen OD1 of D251 [Fig. 6(G)].

More significant changes were observed during the MD simulation of the LIMBS D217A mutant. The LIMBS metal ion immediately (280 ps) moved ~2 Å closer to the MIDAS metal ion [Fig. 6(D)]. Similar to the data of Craig *et al.* for normal αVβ3 in complex with the peptide ligand cilengitide in the presence of Mn^{2+},[32] the side chain of the ligand Asp rotated during the MD simulation in such a way that: (1) the MIDAS metal ion now interacted with the OD1 oxygen [Fig. 6(E), gray line] of the Asp carboxylic group of the ligand rather than OD2 [Fig. 6(F), gray line], and (2) a new contact was formed between the LIMBS metal ion and the carboxylic oxygen OD2 of the ligand Asp [Figs. 5(B) and 6(B)]. Several other changes in the coordination of the β3 metal ions occurred during MD of the D217A mutant: the side-chain of D158 adopted bidentate-like interactions with the LIMBS metal ion, moving its OD1 closer to the LIMBS [Fig. 6(C), gray line], and D251 moved closer to the MIDAS compared with its position in normal αIIbβ3 [Fig. 6(G), gray line]. Water coordination of the metal ions remained the same as it was in the crystal structure during the MD simulations, with two water molecules remaining stably involved in the coordination of the MIDAS ion (see Fig. 5).

Steered molecular dynamics simulations predict that the eptifibatide-αIIbβ3 complex is destabilized only by dissociation of both LIMBS and MIDAS metal ions

We used SMD[31] to investigate the unbinding of eptifibatide from the ligand binding domain of normal αIIbβ3 and the β3 D217A mutant. The computational procedure consisted of applying external steering forces to pull the ligand out of the integrin binding site. Constant velocity pulling was applied to eptifibatide along a predetermined direction (see “Materials and Methods” section), similar to the protocol recently described by Craig et al. for the unbinding of cilengitide from αVβ3.[32] Only the simulations in which a constant pulling velocity of 5 Å/ns was applied are presented because the different pulling velocities provided

qualitatively similar results. It should be noted that even though the absolute values of the calculated forces are not comparable with experimental data because they depend on the particular parameters used in the SMD simulations, the relative values provide insights into the interactions that are responsible for the mechanical stability of the complexes.[32]

Figure 7 depicts the unbinding force-time curves showing the mechanical stabilities of eptifibatide bound to normal αIIbβ3 [Fig. 7(A)] and the β3 D217A LIMBS mutant [Fig. 7(B)] in the presence of the three ions (Ca^{2+}-LIMBS, Mg^{2+}-MIDAS, Ca^{2+}-ADMIDAS), or when one or more of these ions are removed. In normal αIIbβ3 in the presence of all three metal ions [Fig. 7(A), black line], the abrupt reduction in the major force peak observed after ~2500 ps corresponded to the breaking of the interaction of the carboxylic oxygen OD2 atom of the Asp side-chain of eptifibatide with the MIDAS. Removing the LIMBS metal ion from normal αIIbβ3 reduced the force necessary to pull the ligand out of the αIIbβ3 binding site by ~20% (1892 pN vs. 1487 pN) [Fig. 7(A), red line], which is more than the 8% reduction produced by removing the ADMIDAS [1892 pN vs. 1732 pN; Fig. 7(A), green line]. Removing the MIDAS metal ion, or both the MIDAS and LIMBS metal ions, produced greater reductions (48 and 53%) and the disappearance of the peak [Fig. 7(A), blue and cyan lines]. The eptifibatide-pulling simulation in the β3 D217A LIMBS mutant [Fig. 7(B)] in the presence of the three ions (gray line) produced a profile similar to that observed with normal αIIbβ3, with the eptifibatide-MIDAS metal ion interaction breaking at 2069 pN, slightly higher (9%) than the peak observed in the simulation of the normal αIIbβ3 integrin (1892 pN). In agreement with the simultaneous coordination of LIMBS and MIDAS ions by an Asp carboxylic oxygen of eptifibatide in the case of the β3 D217A LIMBS mutant, a second abrupt reduction in the major force peak was observed at ~2750 ps that represented the breaking of the interaction of the second carboxylic oxygen atom of the Asp side-chain with the LIMBS ion. Removing the LIMBS metal ion from the D217A mutant reduced the primary peak of the eptifibatide unbinding force by 37% [Fig. 7(B), red line], a value greater than the 20% observed with normal αIIbβ3. Removing the MIDAS metal ion from the D217A mutant reduced the peak unbinding force by a smaller amount than removing the MIDAS metal ion from normal αIIbβ3 (40% vs. 48%), consistent with the presence of an additional interaction of the ligand Asp with the LIMBS metal ion in the D217A mutant. Note that one out of the two major force peaks remained when only the LIMBS or the MIDAS metal ion was removed. Removing both the LIMBS and MIDAS was required to dramatically reduce the unbinding force [76%; Fig. 7(B), cyan].

Consistent with the findings of Craig *et al.*,[32] water molecules were found to participate actively in the unbinding of eptifibatide from αIIbβ3 by attacking the salt bridges that stabilize the ligand-receptor complex (data not shown). Overall, the attack of water molecules on the ligand Asp oxygen atoms was similar in the unbinding simulations of normal αIIbβ3 and the β3 D217A LIMBS mutant.

DISCUSSION

Functional role of the β3 LIMBS

We carried out cell adhesion experiments on cells expressing normal αIIbβ3, normal αVβ3, and these same receptors carrying either the β3 LIMBS D217A or N215A mutation. Our data demonstrate that alanine mutations of these residues result in virtually complete loss of αIIbβ3-mediated cell adhesion to fibrinogen and the RGD-containing snake venom echistatin, as well as complete loss of αVβ3-specific binding of cells to vitronectin and fibrinogen.

Our data are in accord with: (a) those of Tozer *et al.*, who found that alanine substitution of D217 in αIIbβ3 abolished the binding of both an activation-dependent (PAC1) mAb and an activation-independent (OPG2) ligand mimetic mAb,[13] (b) those of Baker *et al.*, who found that even the relatively conservative mutation D217N decreased PAC1 binding,[14] (c) those of

Yamanouchi *et al.*, who found that a β3 N215A mutant produced a loss of ligand binding to both αIIbβ3 and αVβ3,[17] and (d) those of Cheng *et al.*,[18] who found that a β3 D217H mutation abolished fibrinogen binding to αIIbβ3. They are also in accord with the studies of Pesho *et al.*, who found a dramatic decrease in fibrinogen binding to an isolated β3 βA (I-like) domain containing a D217A mutation at either low or high Ca^{2+} concentrations.[10] The LIMBS in β2 also appears to be absolutely required for ligand binding to αLβ2 and αMβ2, although there are subtle structural differences in the effects of β2 LIMBS mutations depending on the α subunit with which they are paired.[11,15,18] In contrast to these results, and despite the absolute conservation of metal ion coordinating residues between β3 and β7, LIMBS mutations in β7 produced only partial effects on α4β7-mediated ligand binding.[7,9] Therefore, the role of the LIMBS may vary as a function of different α subunits, different ligands, and/or differences in other β3 residues.[7]

Why does the LIMBS play a critical role in ligand binding to β3 integrins?

One of the hypotheses to explain the effect of the β3 LIMBS metal ion on enhancing ligand binding to the MIDAS[5,32] derives from analysis of the integrin crystal structures. Xiong *et al.* noted that the side chain of β3 E220 in the crystal structure of unliganded αVβ3 blocks access of cations to the MIDAS.[5] In the crystal structure of the ligand bound αVβ3, the E220 is further away from the MIDAS as a result of it coordinating the LIMBS Mn^{2+} cation.[5,8] Thus, the LIMBS may allow ligand binding by stabilizing the reorientation of E220 and facilitating the entry of the metal ion into the MIDAS pocket. All of the available crystal structures of αIIbβ3 were obtained in the presence of ligands or a pseudoligand,[8] and they demonstrate the same orientation of E220 as in liganded αVβ3, with coordination of both the LIMBS and MIDAS metal ions. Our MD simulations support the stability of the orientation of the E220 carboxyl oxygen atoms, since we found that the interactions of E220 with both the LIMBS and MIDAS metal ions were maintained throughout the 20-ns interval.

Based on multiple 1 ns MD simulations of the RGD peptide ligand cilengitide bound to αVβ3,[32] Craig *et al.* suggested that the LIMBS ion may also contribute to ligand binding by developing a direct interaction with the ligand Asp carboxylic OD2 oxygen atom. Thus, although the starting crystal structure showed the ligand Asp OD2 oxygen atom coordinating the MIDAS metal ion, within 10 ps of MD, the LIMBS cation moved toward the MIDAS, and the ligand Asp reoriented so that its OD1 oxygen now contributed to the coordination of the MIDAS metal ion and its OD2 atom now coordinated the LIMBS metal ion. The reorientation of the ligand Asp carboxyl oxygens remained stable throughout the remainder of the simulation. In contrast to these findings in αVβ3, our nanosecond time-scale MD simulation of ligand-bound normal αIIbβ3 in the presence of the three β3 metal ions did not show formation of a new contact between the ligand Asp and the LIMBS Ca^{2+} ion at any time during the simulation. A possible explanation for the differences in our findings is that the αIIbβ3 crystal structure we used as the starting structure for our simulation differs from the liganded αVβ3 crystal structure used by Craig *et al.*, in that the β3 D217 in αIIbβ3 is oriented to coordinate the LIMBS. Furthermore, whereas no water molecules were resolved in the αVβ3 structure, two water molecules were resolved coordinating the MIDAS metal ion in the higher resolution αIIbβ3 crystal structure.[8] Thus, the more complete coordination spheres of both the LIMBS and the MIDAS metal ions in the αIIβ3 crystal structure compared with the αVβ3 crystal structure may have affected the likelihood of the ligand Asp carboxyl group rotating toward the LIMBS. Finally, consistent with the importance of the lack of D217 coordination of the LIMBS in the development of the ligand Asp-LIMBS interaction observed by Craig *et al.*, we observed very similar changes in our simulations of the αIIbβ3 D217A LIMBS mutant; thus the eptifibatide Asp carboxyl group rotated toward the LIMBS Ca^{2+} metal ion after only after 1 ps of equilibration run, and then stably coordinated both the MIDAS and LIMBS metal ions thereafter. Of note, substituting a Mg^{2+} metal ion for Ca^{2+} in the LIMBS did not alter the results

of the MD simulations of both normal αIIbβ3 and the corresponding β3 D217A mutant (data not shown).

Our studies also raise the possibility that the LIMBS affects β3 structure in distant regions. In fact, the D217A LIMBS mutant demonstrated increased fluctuations relative to normal αIIbβ3 in the PSI and hybrid domains of β3 as judged by analysis of the MD simulation trajectories of normal αIIbβ3 and the β3 D217A LIMBS mutant (see Fig. 4). However, since we simulated only a portion of the αIIbβ3 structure, it is possible that the differences we observed in dynamic behavior of the portions of β3 that are closest to the attachment to the rest of the β3 chain, namely the hybrid and PSI domains, are not present in the intact receptor. The increased constitutive binding of the LIBS mAb AP5 (which is directed to an epitope on the PSI domain)[22] to the LIMBS mutants (Table I), however, suggests that intact αIIbβ3 receptors also exhibit increased flexibility in this area.

Mechanical stability of the binding to β3 integrins

The results from our SMD simulations of the unbinding of eptifibatide from αIIbβ3 are, overall, in agreement with the SMD simulations of the unbinding of cilengitide from αVβ3 carried out by Craig *et al.*[32] Even though the different contributions to the unbinding force are not entirely correlated in both studies, in both cases the main conclusion is that the interaction of the Asp side-chain of the ligand with the MIDAS is the most important interaction responsible for the mechanical stability of the complex. In fact, one consistent finding in all our SMD studies is that the force necessary to pull the ligand out from the αIIbβ3 integrin binding site is greatest in the presence of all three ions, even for the LIMBS D217A mutant. However, when the LIMBS ion is removed, the peak force is reduced, and it is reduced even more when the MIDAS, or both LIMBS and MIDAS metal ions are removed. The central role of the MIDAS interaction is supported by αIIbβ3 binding studies using a series of echistatin variants[35] that showed that the Asp residue that interacts with the MIDAS is essential for binding, whereas the arginine interaction with the αIIb chain contributes to, but is not required, for integrin recognition by these peptides.[35]

The relationship between ligand binding and metal ion binding to the LIMBS and MIDAS

Our SMD studies demonstrated that the force necessary to pull eptifibatide from the αIIbβ3 integrin was unaffected by the presence of the D217A LIMBS mutation unless accompanied by loss of the LIMBS and/or MIDAS metal ions. Moreover, although loss of the LIMBS metal ion alone reduced the required peak unbinding force, the loss of both the LIMBS and MIDAS metal ions had a much greater impact. Notably, comparable results were obtained when the energy minimized configuration resulting from 20 ns MD simulations of D217A mutant with no LIMBS metal ion in its binding site was used as a starting point for the SMD simulation of eptifibatide unbinding (data not shown). Since our functional studies demonstrated a profound impact of the D217A mutation on ligand binding, it is thus likely that both the LIMBS and MIDAS metal ions are missing in the αIIbβ3 LIMBS D217A mutant of αIIbβ3 integrin. Of note, one previous study of an isolated β3 βA (I-like domain) fragment suggested that producing a D217A mutation in the LIMBS results in loss of the MIDAS metal ion,[16] and a subsequent study of an isolated β3 βA (I-like domain) with a D217A mutation demonstrated lack of binding of the LIMBS ion.[10] Xiong *et al.* also concluded that the binding of the LIMBS metal ion was associated with ligand binding because they did not observe a LIMBS metal ion in the αVβ3 crystals prepared in the presence of either Ca^{2+} or Mn^{2+}, but they did observe it when both Mn^{2+} and the peptide ligand cilengitide was soaked into the crystal prepared in the presence of Ca^{2+}.[4,5] Since ligand binding involves the interaction of a ligand with the MIDAS metal ion, this implies that the LIMBS fills either simultaneously with, or after the MIDAS. On the other hand, the hypothesis that the LIMBS metal ion facilitates and/or stabilizes ligand binding by virtue of its ability to stabilize an orientation of the carboxyl group of E220 out of the MIDAS

pocket suggests that the LIMBS cation binds prior to or simultaneously with the MIDAS. Taken together, these data suggest near simultaneous binding of LIMBS and MIDAS, with each metal ion facilitating and/or stabilizing the binding of the other. Since one of the ligand Asp carboxyl oxygen atoms provides the final coordination site for the MIDAS metal ion, it is likely that the ligand further stabilizes the binding of the MIDAS metal ion. In studies using a program that calculates pathways from the interior of a protein to the bulk solvent (CAVER36), a few potential routes from the LIMBS to the αIIbβ3 surface were identified when using αIIbβ3 conformations obtained by a linear interpolation[37] between the unliganded and liganded structures of αIIbβ3. However, these routes exhibited gorge radii that were either unable to or barely able to accommodate a Ca^{2+} metal ion (ionic radius 0.99) (data not shown). Thus, we favor a model in which the LIMBS fills nearly simultaneously with the MIDAS. Ligand binding to the MIDAS then completes the latter's coordination, and stabilizes the binding of both the MIDAS and the LIMBS.

Acknowledgments

Grant Sponsor: NIH; Grant numbers: HL19278, UL1RR024143; Grant sponsor: Stony Brook University.

Abbreviations

ADMIDAS
adjacent to metal ion-dependent adhesion site

BSA
bovine serum albumin

CPK
Corey-Pauling-Koltun

GMFI
geometric mean fluorescence intensity

HBMT
HEPES-buffered modified Tyrode's solution

HEK
human embryonic kidney

LIBS
ligand-induced binding site

LIMBS
ligand-associated metal binding site

LINCS
linear constraint solver

mAb
monoclonal antibody

MD
molecular dynamics

MIDAS
metal ion-dependent adhesion site

PDBID

protein data bank identification

PME

particle-mesh Ewald

RMSD

root mean square deviation

SMD

steered molecular dynamics

VDW

van der Waals

References

1. Smith JW, Piotrowicz RS, Mathis D. A mechanism for divalent cation regulation of β3-integrins. J Biol Chem 1994;269:960–967. [PubMed: 7507113]
2. Mould AP, Akiyama SK, Humphries MJ. Regulation of integrin α5 β1-fibronectin interactions by divalent cations. Evidence for distinct classes of binding sites for Mn^{2+}, Mg^{2+}, and Ca^{2+} J Biol Chem 1995;270:26270–26277. [PubMed: 7592835]
3. Hu DD, Barbas CF, Smith JW. An allosteric Ca^{2+} binding site on the β3-integrins that regulates the dissociation rate for RGD ligands. J Biol Chem 1996;271:21745–21751. [PubMed: 8702970]
4. Xiong JP, Stehle T, Diefenbach B, Zhang R, Dunker R, Scott DL, Joachimiak A, Goodman SL, Arnaout MA. Crystal structure of the extracellular segment of integrin αVβ3. Science 2001;294:339–345. [PubMed: 11546839]
5. Xiong JP, Stehle T, Zhang R, Joachimiak A, Frech M, Goodman SL, Arnaout MA. Crystal structure of the extracellular segment of integrin αVβ3 in complex with an Arg-Gly-Asp ligand. Science 2002;296:151–155. [PubMed: 11884718]
6. Takagi J, Petre BM, Walz T, Springer TA. Global conformational rearrangements in integrin extracellular domains in outside-in and inside-out signaling. Cell 2002;110:599–511. [PubMed: 12230977]
7. Chen J, Salas A, Springer TA. Bistable regulation of integrin adhesiveness by a bipolar metal ion cluster. Nat Struct Biol 2003;10:995–1001. [PubMed: 14608374]
8. Xiao T, Takagi J, Coller BS, Wang JH, Springer TA. Structural basis for allostery in integrins and binding to fibrinogen-mimetic therapeutics. Nature 2004;432:59–67. [PubMed: 15378069]
9. Chen J, Takagi J, Xie C, Xiao T, Luo BH, Springer TA. The relative influence of metal ion binding sites in the I-like domain and the interface with the hybrid domain on rolling and firm adhesion by integrin α4β7. J Biol Chem 2004;279:55556–55561. [PubMed: 15448154]
10. Pesho MM, Bledzka K, Michalec L, Cierniewski CS, Plow EF. The specificity and function of the metal-binding sites in the integrin β3 A-domain. J Biol Chem 2006;281:23034–23041. [PubMed: 16723352]
11. Chen J, Yang W, Kim M, Carman CV, Springer TA. Regulation of outside-in signaling and affinity by the β2 I domain of integrin αLβ2. Proc Natl Acad Sci USA 2006;103:13062–13067. [PubMed: 16920795]
12. Loftus JC, O'Toole TE, Plow EF, Glass A, Frelinger AL III, Ginsberg MH. A β3 integrin mutation abolishes ligand binding and alters divalent cation-dependent conformation. Science 1990;249:915–918. [PubMed: 2392682]
13. Tozer EC, Liddington RC, Sutcliffe MJ, Smeeton AH, Loftus JC. Ligand binding to integrin αIIbβ3 is dependent on a MIDAS-like domain in the β3 subunit. J Biol Chem 1996;271:21978–21984. [PubMed: 8703003]
14. Baker EK, Tozer EC, Pfaff M, Shattil SJ, Loftus JC, Ginsberg MH. A genetic analysis of integrin function: Glanzmann thrombasthenia in vitro. Proc Natl Acad Sci USA 1997;94:1973–1978. [PubMed: 9050889]

15. Goodman TG, Bajt ML. Identifying the putative metal ion-dependent adhesion site in the β2 (CD18) subunit required for αLβ2 and αMβ2 ligand interactions. J Biol Chem 1996;271:23729–23736. [PubMed: 8798597]

16. Cierniewska-Cieslak A, Cierniewski CS, Blecka K, Papierak M, Michalec L, Zhang L, Haas TA, Plow EF. Identification and characterization of two cation binding sites in the integrin β3 subunit. J Biol Chem 2002;277:11126–11134. [PubMed: 11796735]

17. Yamanouchi J, Hato T, Tamura T, Fujita S. Identification of critical residues for ligand binding in the integrin β3 I-domain by site-directed mutagenesis. Thromb Haemost 2002;87:756–762. [PubMed: 12008962]

18. Cheng M, Foo SY, Shi ML, Tang RH, Kong LS, Law SK, Tan SM. Mutation of a conserved asparagine in the I-like domain promotes constitutively active integrins αLβ2 and αIIbβ3. J Biol Chem 2007;282:18225–18232. [PubMed: 17468108]

19. Coller BS. A new murine monoclonal antibody reports an activation-dependent change in the conformation and/or microenvironment of the platelet glycoprotein IIb/IIIa complex. J Clin Invest 1985;76:101–108. [PubMed: 2991335]

20. Kutok JL, Coller BS. Partial inhibition of platelet aggregation and fibrinogen binding by a murine monoclonal antibody to GPIIIa: requirement for antibody bivalency. J Thromb Haemost 1994;72:964–972.

21. Coller BS, Peerschke EI, Scudder LE, Sullivan CA. A murine monoclonal antibody that completely blocks the binding of fibrinogen to platelets produces a thrombasthenic-like state in normal platelets and binds to glycoproteins IIb and/or IIIa. J Clin Invest 1983;72:325–338. [PubMed: 6308050]

22. Honda S, Tomiyama Y, Pelletier AJ, Annis D, Honda Y, Orchekowski R, Ruggeri Z, Kunicki TJ. Topography of ligand-induced binding sites, including a novel cation-sensitive epitope (AP5) at the amino terminus, of the human integrin β3 subunit. J Biol Chem 1995;270:11947–11954. [PubMed: 7538128]

23. Nelson EJ, Li J, Mitchell WB, Chandy M, Srivastava A, Coller BS. Three novel β-propeller mutations causing Glanzmann thrombasthenia result in production of normally stable pro-αIIb, but variably impaired progression of pro-αIIbβ3 from endoplasmic reticulum to Golgi. J Thromb Haemost 2005;3:2773–2783. [PubMed: 16359515]

24. Law DA, Nannizzi-Alaimo L, Ministri K, Hughes PE, Forsyth J, Turner M, Shattil SJ, Ginsberg MH, Tybulewicz VL, Phillips DR. Genetic and pharmacological analyses of Syk function in αIIbβ3 signaling in platelets. Blood 1999;93:2645–2652. [PubMed: 10194444]

25. Berendsen HJC, van der Spoel D, van Drunen R. GROMACS: A message-passing parallel molecular dynamics implementation. Comput Phys Commun 1995;91:43–56.

26. Van Der Spoel D, Lindahl E, Hess B, Groenhof G, Mark AE, Berendsen HJ. GROMACS: fast, flexible, and free. J Comput Chem 2005;26:1701–1718. [PubMed: 16211538]

27. Humphrey W, Dalke A, Schulten K. VMD: visual molecular dynamics. J Mol Graph 1996;14:27–38. 33–38.

28. Darden T, York D, Pedersen L. Particle mesh Ewald: an N-log(N) method for Ewald sums in large systems. J Chem Phys 1993;98:10089–10092.

29. Hess B, Bekker H, Berendsen HJC, Fraaije JGEM. LINCS: A linear constraint solver for molecular simulations. J Comput Chem 1997;18:1463–1472.

30. Berendsen, HJC.; Postma, JPM.; Gunsteren, WF.; Hermans, J. Interaction models for water in relation to protein hydration. In: Pullman, B., editor. Intermolecular forces. Dordrecht: Reidel; 1981. p. 331-342.

31. Isralewitz B, Gao M, Schulten K. Steered molecular dynamics and mechanical functions of proteins. Curr Opin Struct Biol 2001;11:224–230. [PubMed: 11297932]

32. Craig D, Gao M, Schulten K, Vogel V. Structural insights into how the MIDAS ion stabilizes integrin binding to an RGD peptide under force. Structure 2004;12:2049–2058. [PubMed: 15530369]

33. Gan ZR, Gould RJ, Jacobs JW, Friedman PA, Polokoff MA. Echistatin. A potent platelet aggregation inhibitor from the venom of the viper, *Echis carinatus*. J Biol Chem 1988;263:19827–19832. [PubMed: 3198653]

34. Savage B, Marzec UM, Chao BH, Harker LA, Maraganore JM, Ruggeri ZM. Binding of the snake venom-derived proteins applaggin and echistatin to the arginine-glycine-aspartic acid recognition

site(s) on platelet glycoprotein IIb. IIIa complex inhibits receptor function. J Biol Chem 1990;265:11766–11772. [PubMed: 2365698]

35. Hantgan RR, Stahle MC, Connor JH, Horita DA, Rocco M, McLane MA, Yakovlev S, Medved L. Integrin αIIbβ3: ligand interactions are linked to binding-site remodeling. Protein Sci 2006;15:1893–1906. [PubMed: 16877710]
36. Petrek M, Otyepka M, Banas P, Kosinova P, Koca J, Damborsky J. CAVER: a new tool to explore routes from protein clefts, pockets and cavities. BMC Bioinformatics 2006;7:316. [PubMed: 16792811]
37. Krebs WG, Gerstein M. The morph server: a standardized system for analyzing and visualizing macromolecular motions in a database framework. Nucleic Acids Res 2000;28:1665–1675. [PubMed: 10734184]

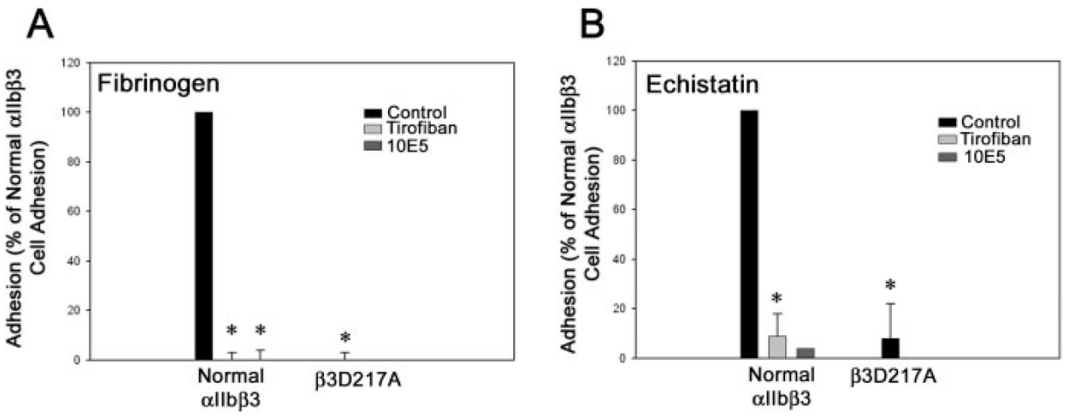

Figure 1.

A β3 D217A LIMBS mutation in αIIbβ3 results in defective adhesion to fibrinogen and echistatin. HEK293 cells expressing normal αIIbβ3 or β3 D217A LIMBS were allowed to adhere to wells coated with (**A**) fibrinogen or (**B**) echistatin in the presence of 100 μM Ca^{2+} and 50 μM Mg^{2+}, with or without 20 μg/mL of the αIIbβ3-specific mAb 10E5, or 100 μM of the αIIbβ3 inhibitor tirofiban. Surface expression of αIIbβ3, measured by flow cytometry using anti-αIIb mAb HIP8 and expressed as GMFI (mean ± SD; n = 3) was 122 ± 21 for normal αIIbβ3 and 116 ± 23 for D217A. Results are presented as percentages of the adhesion of cells expressing normal αIIbβ3 [(mean ± SD); n = 3, except for adhesion to echistatin in the presence of mAb 10E5 where n = 1]. *P < 0.001 when compared with cells expressing normal αIIbβ3 receptor.

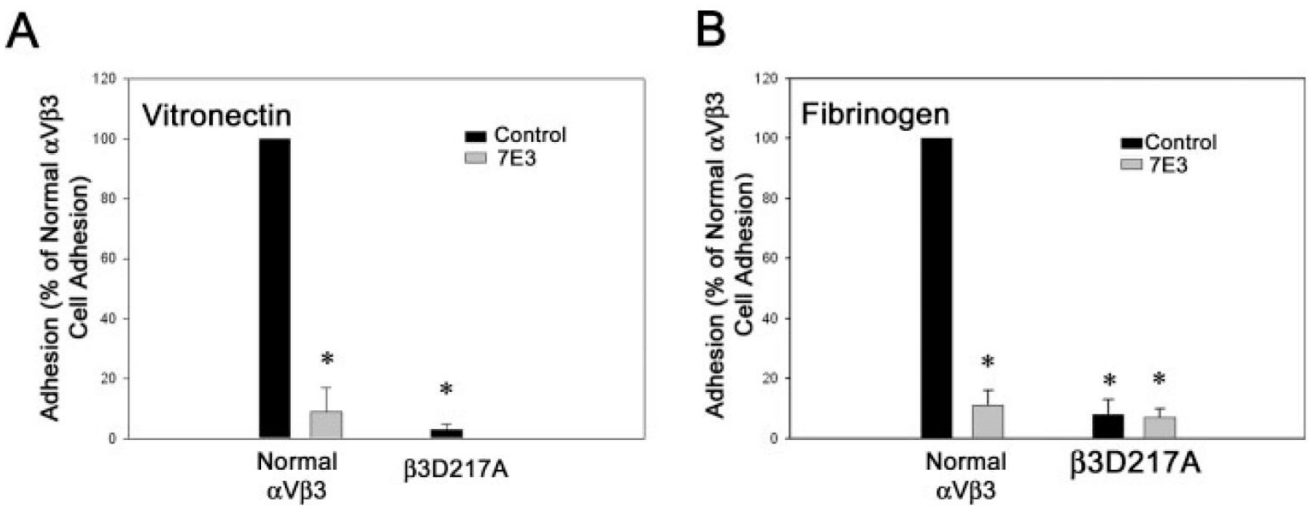

Figure 2.

A β3 D217A LIMBS mutation in αVβ3 results in impaired adhesion to vitronectin and fibrinogen. CS-1 cells expressing normal αVβ3 or a β3 D217A mutant αVβ3 were allowed to adhere to vitronectin-coated wells in the presence of 1 mM Mg^{2+} (**A**) or to fibrinogen-coated wells in the presence of 0.5 mM Mn^{2+} (**B**) with or without 20 μg/mL of the inhibiting mAb 7E3. Surface expression of αVβ3 receptors, measured by the binding of the β3 mAb 7H2, was 22 ± 1, for the normal and 17 ± 3 for the D217A mutant (GMFI mean ± SD). Results are expressed as in Figure 1; n = 3. *P < 0.001 when compared with cells expressing the normal αVβ3 receptor.

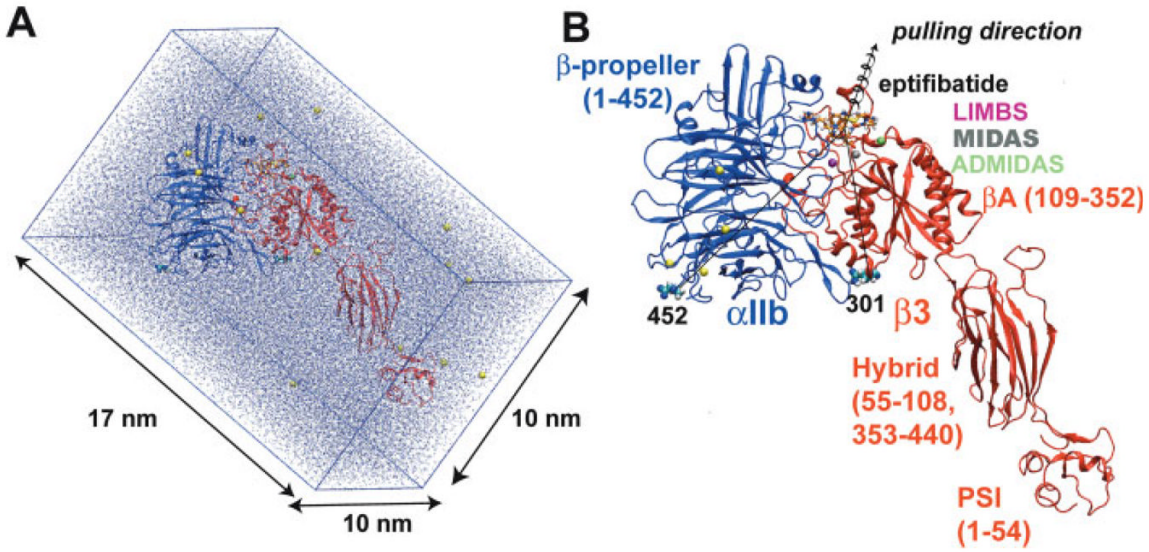

Figure 3.

System setup for the equilibrium and nonequilibrium (steered) MD simulations of normal αIIbβ3 and the β3 D217A αIIbβ3 mutant in complex with eptifibatide. (**A**) Initial structure of the normal complex (ribbon representation) in the orthogonal unit cell (solid lines) used to simulate the system with periodic boundary conditions. The system is solvated in water (blue dots). Sodium counterions used to neutralize the systems are shown in van der Waals (VDW) representations in yellow color. (**B**) Ribbon representation of normal αIIbβ3 in complex with eptifibatide (PDBID: 1TY6) depicting the domains considered in our simulations and the corresponding residue numbers. Eptifibatide (orange) is shown in licorice representation. Metal ions occupying the LIMBS, MIDAS, and ADMIDAS sites of the β3 chain are shown in purple, gray, and green VDW representations, respectively. The pulling direction chosen for the SMD simulations of the unbinding of eptifibatide from the αIIbβ3 RGD binding site is indicated with a black arrow. Vectors defining this direction are indicated with black lines, while the residues from which these vectors originate (452 of αIIb and 301 of β3) are depicted as Corey-Pauling-Koltun (CPK) representations.

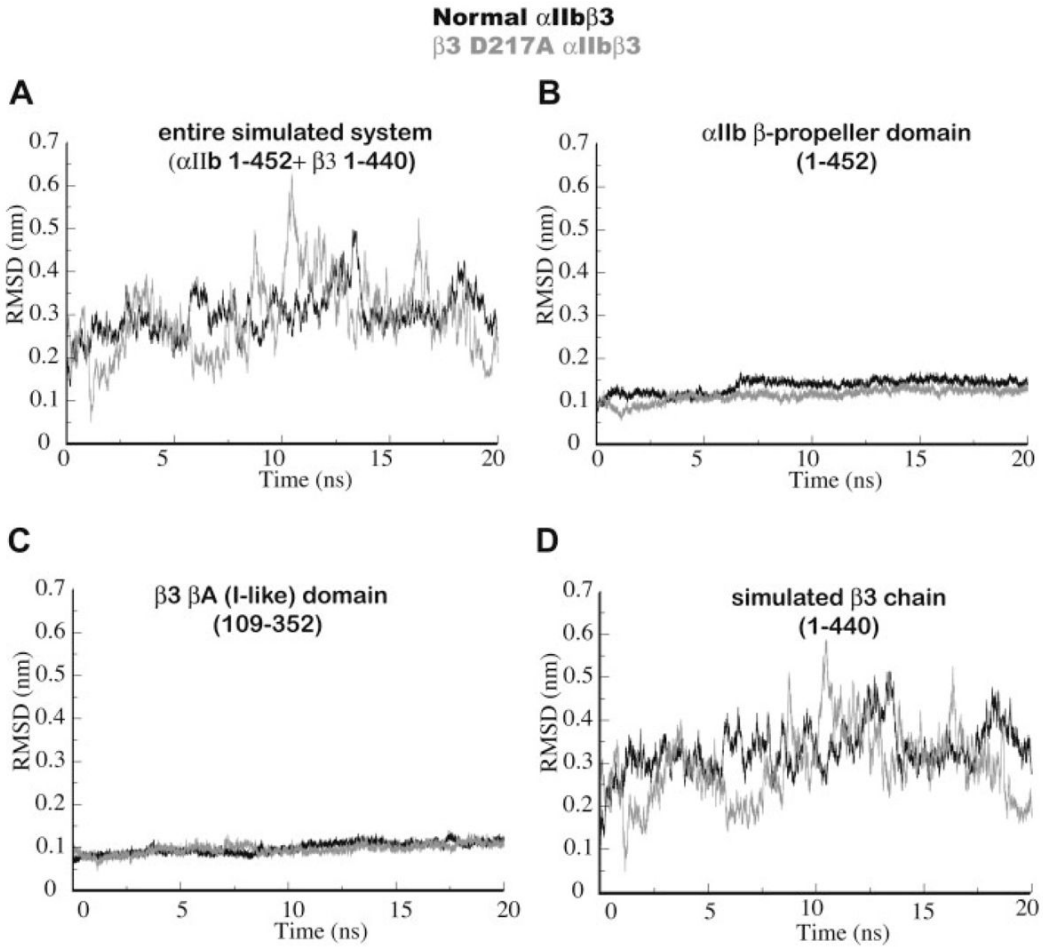

Figure 4.

Time evolution of the RMSD of the Cα atoms of normal αIIbβ3 integrin (black) and the β3 D217A LIMBS mutant (gray) with respect to each corresponding initial structure. RMSDs are calculated for the following: (**A**) the entire simulated system, (**B**) the αIIb β-propeller domain, (**C**) the β3 βA (I-like) domain, or (**D**) the β3 chain (1–440), including the βA (I-like), PSI, and hybrid domains.

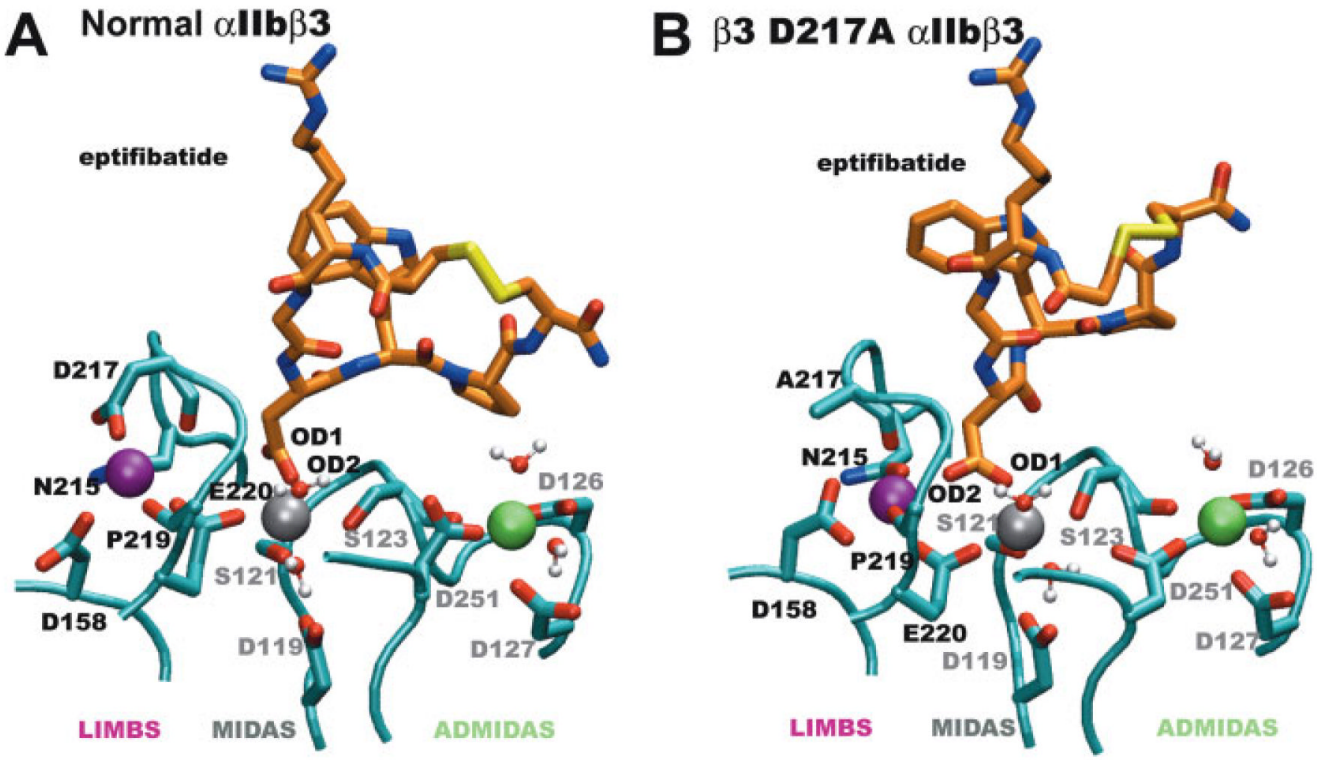

Figure 5.

Close-up view of the eptifibatide binding site in (**A**) normal αIIbβ3 and (**B**) the β3 D217A LIMBS mutant at the end of simulations. Eptifibatide (orange) and ion coordinating residues (cyan) are shown in licorice style; LIMBS (purple), MIDAS (gray), and ADMIDAS (green) cations are in VDW; and coordinating water molecules are in CPK. Hydrogen atoms of the side-chains and ligand are omitted for clarity.

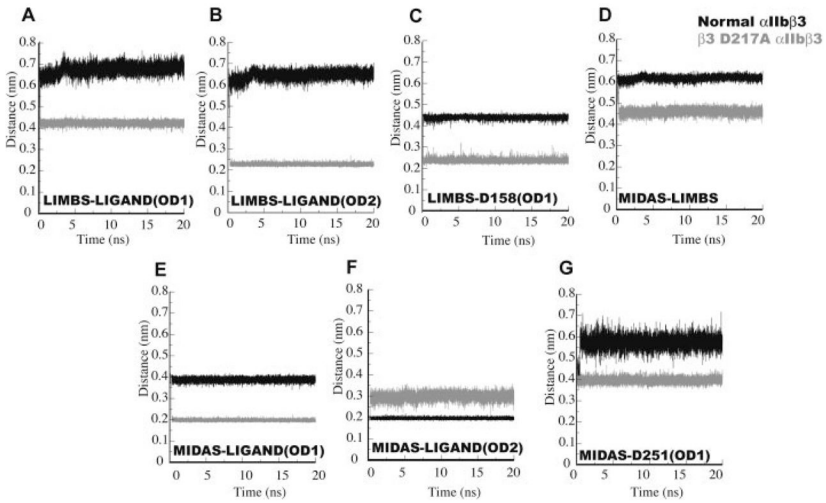

Figure 6.

Distances between the integrin coordinating residues and LIMBS and MIDAS ions that differed by more than 1 A ° in normal αIIbβ3 (black) and the β3 D217A mutant (gray) during MD simulations, as well as between the metal ions. Reported distances are as follows: (**A**) between the LIMBS metal ion and the ligand Asp carboxylic oxygen OD1; (**B**) between the LIMBS metal ion and the ligand Asp carboxylic oxygen OD2; (**C**) between the LIMBS metal ion and the carboxylic oxygen OD1 of the β3 residue D158; (**D**) between MIDAS and LIMBS metal ions; (**E**) between the MIDAS metal ion and the ligand Asp carboxylic oxygen OD1; (**F**) between the MIDAS metal ion and the ligand Asp carboxylic oxygen OD2; (**G**) between the MIDAS metal ion and the carboxylic oxygen OD1 of the β3 residue D251.

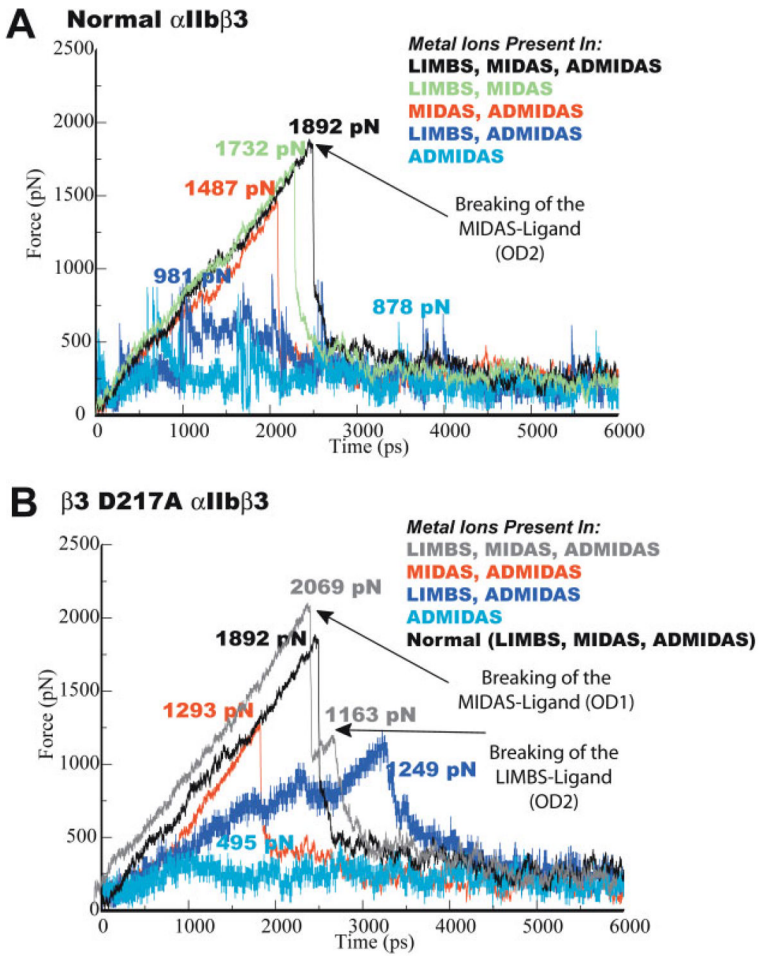

Figure 7.

SMD force profiles of the unbinding of eptifibatide from (**A**) normal αIIbβ3, and (**B**) β3 D217A mutant before and after removing the interaction with one or more metal ions.

Table I

AP5 Binding to Normal αIIbβ3 and β3 LIMBS Mutants in the Presence and Absence of EDTA

β3 subunit	AP5 binding[a] (no EDTA)	AP5 binding[a] (with EDTA)	Ratio ± EDTA
Normal	5 (2–7)	40 (21–103)	8
N215A	31 (18–43)*	87 (51–195)	3
D217A	23 (14–43)*	65 (48–115)	3

Expression of αIIbβ3 on the normal and mutant cells was assessed by the binding of fluorescently labeled mAb HIP8 (anti-αIIb). For normal αIIbβ3, the β3 N215A, and β3 D217A mutants, the geometric mean fluorescent intensity (GMFI) values were 134 ± 33, 113 ± 48, and 126 ± 57, respectively (mean ± SD, $n = 12$).

[a] AP5 binding expressed as percentage of HIP8 binding. Data are presented as median (25th–75th percentile), and were obtained from 12 separate experiments in the absence of EDTA and 6 experiments in the presence of EDTA. Ratio data are from 6 experiments in which both values were obtained.

* $P < 0.001$ when compared with normal.

Table II

AP5-Induced Binding of Soluble Fibrinogen to Cells Expressing Normal αIIbβ3 and αIIbβ3 β3 LIMBS Mutants

β3 subunit	Fibrinogen binding (baseline)	Fibrinogen binding (with AP5)	N
Normal	11 ± 4	38 ± 22*	4
N215A	8 ± 1	8 ± 2	3
D217A	9 ± 2	9 ± 2	3

Fluoresecent fibrinogen binding was induced by incubation with 60 μg/ml AP5 in the presence of 2 mM Ca^{2+} and 1 mM Mg^{2+} for 30 min at 37°C. Surface expression of αIIbβ3, as assessed by the binding of mAb HIP8 (anti-αIIb), was 155 ± 37, 91 ± 10, and 202 ± 18, respectively (mean GMFI ± SD). Results are presented as mean GMFI ± SD.

* $P = 0.04$ baseline versus in the presence of AP5.